AD-A270 041

TION PAGE

1. AGENCY USE ONLY *(Leave blank)*	2. REPORT DATE	3. REPORT TYPE AND DATES COVERED
	May 1993	Professional Paper

4. TITLE AND SUBTITLE

COUPLED NEURAL-DENDRITIC PROCESSES; COOPERATIVE STOCHASTIC EFFECTS AND THE ANALYSIS OF SPIKE TRAINS

5. FUNDING NUMBERS

PR: MA57
PE:
WU:

6. AUTHOR(S)

7. PERFORMING ORGANIZATION NAME(S) AND ADDRESS(ES)

Naval Command, Control and Ocean Surveillance Center (NCCOSC)
RDT&E Division
San Diego, CA 92152-5001

8. PERFORMING ORGANIZATION REPORT NUMBER

9. SPONSORING/MONITORING AGENCY NAME(S) AND ADDRESS(ES)

10. SPONSORING/MONITORING AGENCY REPORT NUMBER

11. SUPPLEMENTARY NOTES

12a. DISTRIBUTION/AVAILABILITY STATEMENT

Approved for public release; distribution is unlimited.

12b. DISTRIBUTION CODE

13. ABSTRACT *(Maximum 200 words)*

We can create a richer and more neurophysiologically realistic model of neural activity in the brain by developing a model of neural-dendritic coupling, one which expressly accounts for the way in which the many afferent connections into the neural body influence the somatic membrane potential. Such a model would begin to fill the need within the Artificial Neural Network community for neural models which go beyond the current "weighted sum" paradigm for artificial neuron connectivity. Although such models have use in engineering applications, there are many aspects of biological neural-dendritic organization which could enrich artificial neural networks. Moving from simple "axonal" connection weight neural models to neural-dendritic models with a richer structure will allow investigation of both events at the neural level (e.g., inter-spike interval histograms and stochastic resonance) and also potentially at the neural systems level. This will also introduce the possibility of introducing cross-scale interactions into artificial neural systems.

Published in *Proceedings First Appalachian Conference on Behavioral Neurodynamics: Processing in Biological Neural Networks*.

14. SUBJECT TERMS	15. NUMBER OF PAGES
	16. PRICE CODE

17. SECURITY CLASSIFICATION OF REPORT	18. SECURITY CLASSIFICATION OF THIS PAGE	19. SECURITY CLASSIFICATION OF ABSTRACT	20. LIMITATION OF ABSTRACT
UNCLASSIFIED			SAME AS REPORT

21a. NAME OF RESPONSIBLE INDIVIDUAL	21b. TELEPHONE (include Area Code)	21c. OFFICE SYMBOL
A. Bulsara	(619) 553-1595	Code 573

DISCLAIMER NOTICE

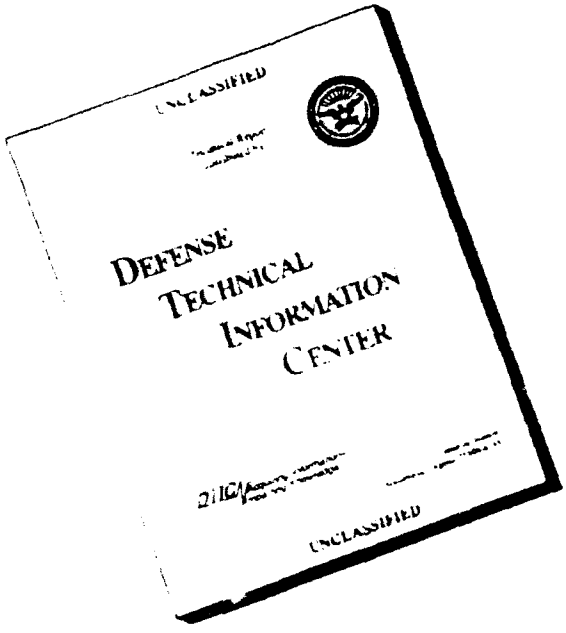

THIS REPORT IS INCOMPLETE BUT IS THE BEST AVAILABLE COPY FURNISHED TO THE CENTER. THERE ARE MULTIPLE MISSING PAGES. ALL ATTEMPTS TO DATE TO OBTAIN THE MISSING PAGES HAVE BEEN UNSUCCESSFUL.

COUPLED NEURAL-DENDRITIC PROCESSES; COOPERATIVE STOCHASTIC EFFECTS AND THE ANALYSIS OF SPIKE TRAINS

A. R. Bulsara

NCCOSC-RDT&E Division, San Diego, CA 92152

A. J. Maren

Accurate Automation Corp., 1548 Riverside Drive, Chattanooga, TN 37406
and
Brain Research Center and Computer Sciences Dept., Radford University,
Radford, VA 24142

ABSTRACT

We can create a richer and more neurophysiologically realistic model of neural activity in the brain by developing a model of neural-dendritic coupling, one which expressly accounts for the way in which the many afferent connections into the neural body influence the somatic membrane potential. Such a model would begin to fill the need within the Artificial Neural Network community for neural models which go beyond the current "weighted sum" paradigm for artificial neuron connectivity. Although such models have use in engineering applications, there are many aspects of biological neural-dendritic organization which could enrich artificial neural networks. Moving from simple "axonal" connection weight neural models to neural-dendritic models with a richer structure will allow investigation of both events at the neural level (e.g. inter-spike interval histograms and stochastic resonance) and also potentially at the neural systems level. This will also introduce the possibility of introducing cross-scale interactions into artificial neural systems.

I. INTRODUCTION

The effect of neural-dendritic interactions has so far been only weakly probed in the realm of artificial neural networks and neural modeling. Traditional Artificial Neural Network (ANN) models of interacting neurons use a simple description of neural connectivity. In such simple models, communication between neurons is afforded by artificial axons, and the "strength" of a given neuron-to-neuron connection is given as a "connection weight" between the two neurons. Synaptic plasticity is viewed in terms of the modifiability of connection weight ("axonal") strengths (for a review of ANNs, see Maren, Harston, and Pap, 1990).

A more neurophysiologically realisitic - and interesting - basis for modeling neural systems would take into account the nature of neural-dendritic connectivity. Such considerations for neural systems modeling were advanced as early as 1958 by John von Neumann. In 'The Computer and the Brain,' von Neumann wrote:

> ...However, the more frequent situation is that the body of a neuron has synapses with axons of many other neurons. It even appears that, occasionally, several axons from one neuron form synapses on another. Thus the possible stimulators are many, and the patterns of stimulation that may be effective have more complicated definitions than the simple "and" and "or" schemes described ... It may well be that certain nerve pulse combinations will

second-order chemically gated synapses have longer time constants and cannot be treated by our model.

In order to characterize processes at the synaptic level, i.e., to characterize a dendritic volume activation in terms of its relationships to inputs and to activation decay, we set $a_i(t)$ to be the total post-synaptic activation of a small *dendritic volume*, which can include several dendritic spines and their afferent connections. The dendritic volume is roughly equivalent to the "dendron" introduced by Eccles [1964]. Pre-synaptic chemically-gated input to the dendritic volume, resulting from action potentials at other neurons, contributes to the total dendritic volume activation. We think of this input as being predominantly due to chemically-gated synaptic transmissions which have time-constants in the 1-5ms. range [Kandel et. al. 1991 pg. 124]. To a great extent, the elicited post-synaptic-potential (PSP) response to afferent spiking is linear. However, the response is bounded from above in the case of excitatory inputs and from below when the inputs are inhibitory. This is due to probabilistic release of quantized packets of neurotransmitter into the synaptic cleft [Eccles, 1981] and to a finite number of channels in the post-synaptic terminus. Further, experimental measurements of excitatory and inhibitory PSPs show that both are maximally within several tens of millivolts of the membrane resting potential [Kandel et. al. 1991]. This also indicates bounding of the PSPs. Bounding also comes about through scalingof the PSP which occurs in the short distance the PSP travels from the synaptic site, at the spine head, to the spine base; simulations indicate that the potential may drop by as much as 95% as a result [Segev et. al. 1992]. Consideration of these combined factors will allow us to model the temporal derivative of the activation or total polarization of a small dendritic volume as an activation decay term plus input terms. The inputs will include the weighted and bounded effects of presynaptic signals from axonal and/or dendritic connections, a weak (low amplitude and frequency) periodic driving force, and noise. As we shall see later, the form for the temporal derivative of the activation in a synaptic volume will be the same as for the neural body itself.

The activation potential which originates in a local dendritic volume and moves through the dendritic arborization towards the soma undergoes two substantial changes [Segev et. al. 1992]. Both changes influence the model that we construct for time-dependent activation at the soma. First, there is a marked attenuation of the maximal signal amplitude, and second, there is a drawing out of the signal waveform. Simulations by Rall and Rinzel [1973], Rinzel and Rall [1974] and Segec et. al. [1992] indicate a strong attenuation if the synaptic PSP as it passes from the originating dendritic volume towards the soma. The final maximal signal amplitude reaching the soma can be less than 1% of the original maximal amplitude, even though the stretched signal duration indicates that a substantial portion of the signal is preserved via temporal integration. This leads us to model the neuronal (i.e. soma) input not as the direct value of the synaptic activation but rather as a bounded function of it. This makes plausible the use of a transfer function such as a sigmoid or hyperbolic tangent, which is so ubiquitous in neural modeling. It is important to point out that the decoupling (to be described in the following section) of the neuro-dendritic stochastic differential equations via the adiabatic theory will be tantamount to a "quasi-linearization" of the dendritic dynamics. Another observation arising out of these simulations is that the PSP signal waveform is greatly stretched as it travels towards the soma. Specifically, an input that may occur in less than $10ms.$ at the synaptic site may have an influence persisting over $100ms.$ at the soma. This is particularly true if the synaptic site is far from the soma. We can summarize this by noting that "...the dendritic tree behaves as a substantial *delay line* for the synaptic inputs [and that] distal inputs are subject to significantly longer neural delays than proximal inputs..." [Segev et. al. 1992]. The notion of different distributions of synaptic input has been stated and experimentally observed as early as the 1960s [e.g. Rall 1970]. In any given neuron, due to the branching nature of the dendritic tree, there will be far more distal inputs than proximal inputs. Thus, to a first approximation, we can model the synaptic inputs under the assumption that the time-constants of events are "stretched" as they move through the dendritic passage to the soma. This allows us to make an adiabatic approximation in treating the activation equations of the dendritic volumes and the neuron.

We turn our attention now to the membrane potential at the neural soma and axon hillock, and note that again we may think of the temporal derivative of the activation as the sum of an

back to a (zero-level) resting state. A more effective model of neural activation requires that the inputs to the neural system be modeled in a continuous manner, consistent with our understanding of the "stretched" arrival of dendritic activations at the neural soma, as has been described by Rall and Rinzel [1973], Rinzel & Rall [1974], Holmes & Rall [1992], and Segev et al. [1992]. In a later work, Stein et al. [1974] identified the activation of the neuron as the rate at which nerve impulses would be fired. While this would allow an intuitive connection between the neural model description and "states", which could be roughly described in terms of the average frequency of firing of an action potential, it does not serve when the model needs to be connected with a more explicit description of neural dynamics, such as the generation of interspike interval histograms. We will return to this point later in this work. Subsequent investigators have developed diffusion models in which the discontinuities in $u_1(t)$ have been smoothed out (see e.g. Tuckwell, 1980 and references cited therein). While more mathematically tractable, such models again treat the arrival of excitatory and inhibitory signals to the neural soma as discrete rather than continuous processes.

For the current work, a more precise identification of the neural membrane potential is needed; one which distinguishes it from the potentials within the dendritic network afferent to the soma, and one which decouples the continuous-time activation changes in the soma that occur in response to input and activation decay from the action potential, whose abrupt nature may be viewed as a reset mechanism of an otherwise continuous process. In our work, the variable $u_1(t)$ refers specifically to the membrane potential at the trigger zone in the neural soma. This is because the interesting dynamics of the soma are generated at the trigger zone, which has a lower threshold than the rest of the soma. However, changes in membrane potential at the trigger zone propagate rapidly both throughout the soma itself, and down the axon as an action potential. We regard the brief depolarization and ensuing hyperpolarization of the action potential (and its corollary within the neural soma itself) as a reset mechanism whose details are not addressed in this work. Our model does, however, address the continuous changes in membrane potential due to dendritic connectivity, activation decay, and other factors.

The disparity in the neural and dendritic time-constants discussed above is incorporated into our model via the constraint,

$$R_i \ll R_1 \quad (i>1). \tag{2}$$

This constraint will allow us to confidently utilize the slaving principle of Haken [1977] to reduce the system (1). This reduction is carried out in the next section. We also consider, via numerical simulations, the range of validity of the adiabatic elimination technique as well as the bifurcation properties and collective effects that appear in the decoupled neuron dynamics because of the interaction with the dendritic bath. Finally, we discuss switching events (between the firing/quiescent states of the neuron) that arise as a consequence of the interplay between the noise and the periodic modulation... *stochastic resonance*.

II. SINGLE NEURON DYNAMICS

The separation of time-scales embodied in the inequality (2) permits us to apply the slaving principle [Haken 1977] to the coupled system (1). This leads to a closed equation for the soma activation function $u_1(t)$ i.e., the system (1) is decoupled. The proceedure is outlined in the following subsection (refer to Schieve, Bulsara and Davis 1991, Bulsara, Maren and Schmera, 1992 for details) in which we also introduce the effective "potential function" corresponding to the single neuron dynamics. This is followed by an analysis of the bifurcation properties of the reduced model (in the absence of the deterministic modulation $q\sin\omega t$). The remainder of this paper examines the cooperative effects (together with their potential implications in neuroscience) that arise when this modulation term is switched on.

Reduced Neuron Equation

Equation (1) represents a system of globally coupled nonlinear stochastic differential equations, subject to the constraint (2) on the equivalent circuit resistors R_i. The N-dimensional

where $\sigma_i^2 \equiv \sigma_i^2 / C_i^2$ and $F(t)$ is Gaussian delta-correlated noise having zero mean and unit variance and we have introduced the (deterministic) potential function that affords us a more elegant mathematical treatment of the dynamics:

$$U(u_1) = \frac{1}{2}\alpha u_1^2 - \beta \ln \cosh u_1 \tag{10}$$

The coefficients in the above dynamics are given by,

$$\alpha \equiv (R_1 C_1)^{-1} \tag{11a}$$

$$\beta \equiv C_1^{-1} \left[J_{11} + \sum_{i>1} R_i G_i^{-1} J_{1i} J_{i1} \left[1 - \frac{\sigma_i^2 R_i}{2C_i} \right] \right], \tag{11b}$$

$$\delta \equiv \frac{q}{C_1} \left[1 + \sum_{i>1} R_i G_i^{-1} J_{1i} \left[1 - \frac{\sigma_i^2 R_i}{2C_i} \right] \right], \tag{11c}$$

and we have set $G_k \equiv 1 - J_{kk} R_k$. Equation (9) (the so-called "reduced" or "effective" neuron dynamics) constitutes the starting point for our subsequent analyses, u_1 representing the voltage at the soma. We note that it contains (via (11)) the effects of the coupling between the cell body and each of the dendritic volumes. Back-coupling (characterized by the coefficients J_{i1}) effects are included as well as self-feedback terms (characterized by the coefficients J_{ii}). Cross-coupling terms (characterized by products of the form $R_i R_k J_{ik} J_{ki}$; $k, i > 1$) between the dendritic spaces are also present but are neglected. It is important to point out that, in general, the expressions (11b,c) contain higher order terms; these are absent because of the truncation (at second order) of the Taylor expansion of the functions $\tanh u_{i>1}$, consistent with our assumption of small deviations from equilibrium of the dendritic "bath". The detailed analysis [Schieve, Bulsara and Davis 1991] leading up to the expressions (11) shows these terms to be of higher order in $\sigma_i^2 R_i / 2C_i$. We assume that the dendritic noise terms are sufficiently weak so that we always have

$$\frac{\sigma_i^2 R_i}{2C_i} < 1 \quad i > 1, \tag{12}$$

so that the deviations $u_i - \bar{u}_i$ are small. Note also that we have *not* assumed that the matrix J is symmetric, in contrast with existing (Hopfield-type) models. In fact, no further assumptions beyond (2) and (12) (both of which are based on very reasonable physical and neurophysiological arguments) as well as the adiabatic assumption of very low modulation frequency ω need be made to obtain the reduced neuron dynamics (9). In the next subsection, we write down the "potential" function corresponding to the reduced neuron dynamics and examine its stability and bifurcation properties. We also present numerical simulation results that elucidate the range of validity of the reduced description (9) when compared to the full dynamics (1).

Steady-State Potential Function; Stability and Bifurcation Properties

It is easy to show, via linear stability analysis, that the dynamics in (9) are globally stable as long as $\alpha \geq 0$. For this case, the potential function $U(u_1)$ is a Liapounov function for the reduced dynamics (9). We note that stability does *not* depend on the properties of the coupling matrix J. Assuming $\alpha \geq 0$, we can easily show that the potential (10) will be parabolic (with an elliptic fixed point at $u_1 = 0$) if $\beta \leq \alpha$ (this includes negative as well as positive values of β). For $\beta > \alpha$, the potential is bimodal (with its minima located at $c = \pm(\beta/\alpha)\tanh(\beta/\alpha)$, and a hyperbolic fixed point at $c = 0$) and cooperative stochastic effects come into play. The transition to bimodality (at $\beta = \alpha$) is accompanied by a pitchfork bifurcation in the most probable value of the activation u_1 with the two states (attractors) corresponding roughly to the quiescent and firing states of the neuron. The flow (given by the first term on the rhs of (9)) exhibits the characteristic N-shaped relationship known to exist in excitable cells (see e.g. Rinzel and Ermentrout 1989; Abbott and Kepler 1990). We now consider the effects of the cell body coupling to multiple dendritic volumes on this transition. Throughout the remainder of this work we shall assume, for simplicity, that the noise variances in the elemental dendritic volumes are the same and, further, that all the dendritic time constants are equal. Specifically, we set $\sigma_i^2 = \sigma_2^2, R_i = R_2$ for all $i > 1$ and $C_i = 1$ for all i. We also

We now digress briefly to consider the case in which the potential is monomodal in the absence of any coupling to the dendritic bath (this can be achieved by setting $J_{ik}R_2 < 1$), in contrast to the case discussed in the preceding paragraph. Then, one can easily calculate the value of R_2 (for given noise variance σ_2^2 and configuration of the matrix $\mathbf{J}$) above which the effective potential is bimodal. Increasing R_2 leads to a transition to bimodality (occurring at $\beta\alpha=1$) *only* for the case in which the sum $\sum_{i\neq k} J_{ik}J_{ki}$ is positive (keeping in mind the constraint imposed by the inequality (12)). This may be realized by imposing the same sign on the vast majority of the off-diagonal elements J_{ik} and J_{ki}. Increasing the noise variance σ_2^2 degrades the effect; this is evident from (11b). It is apparent that the coupling to the dendritic bath may actually introduce a phase-transition-like behavior into the neuron dynamics. Effects such as this *coupling-induced bimodality* are a hallmark of multiplicative noise (see e.g. Horsthemke and Lefever 1984) and have been examined in simpler neuron models (for both additive and multiplicative noises) by Bulsara, Boss and Jacobs [1989], and Bulsara and Schieve [1991]. The opposite effect can also occur: depending on the magnitude and sign of each element J_{ij}, a potential that is bistable in the absence of the bath coupling, can be rendered monostable by the dendritic field. This is evident from (11b).

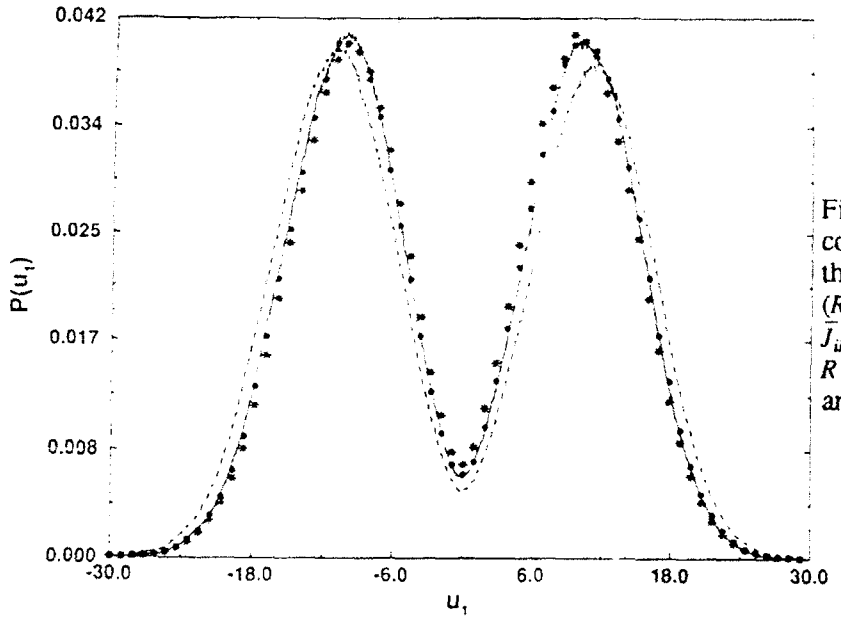

Fig 2. Neuron (cell body) probability density computed via direct integration of (1) and the reduced equation (9) (data points). $(R_1,\sigma_1^2,\sigma_2^2,q,\omega,N)\equiv(10,5,2,0.1,0.1,10)$. $\bar{J}_{ik}=1=J_{ik}^2$, $\bar{J}_{ii}=0$, $J^2=1$ $(i>1)$. $R_2=0.35$ (solid curve and filled data points) and 1.0 (dashed curve and asterisk data points).

Before concluding this subsection, we present the results of numerical simulations aimed at demonstrating the validity of the approximations made in this paper. Figure 2 shows the probability density function corresponding to the "slow" variable u_1. The solid curves (corresponding to simulations of the fully coupled system (1)) have been obtained via direct integration on an HP-Apollo 425T workstation. We consider $N=10$ elements since the simulations become prohibitively time-consuming for larger N values. The system has been integrated through 12,000 periods of the deterministic modulation (after allowing the transients to die out) using a stepsize of 0.015. Noise has been included in the dynamics via the Heun algorithm (see e.g. Greiner et. al. 1988). The data points show the results of integrating the corresponding effective one-body equation (9) using the same routine. In this figure we take $R_1=10$ and consider the case $R_2=0.35$ and 1.0, all other parameters remaining fixed. The agreement between the exact and reduced dynamics is seen to be excellent for $R_2=0.35$. Increasing R_2 to 1.0 still yields reasonably good qualitative agreement although it is apparent that we are very close to the boundary at which (2) ceases

An approximate expression for the power spectral density for a one-dimensional nonlinear stochastic system of the form (9) has been derived by McNamara and Wiesenfeld [1989]:

$$P(\Omega) = [1 - 2Z(r_0\zeta)^2](8Zr_0c^2) + 4Z\pi(r_0\zeta c^2)^2\delta(\Omega-\omega)$$
$$\equiv \mathbf{N}(\Omega) + \mathbf{S}(\Omega)\delta(\Omega-\omega), \tag{16}$$

where we define $Z = (4r_0^2 + \Omega^2)^{-1}$ and $\zeta = \delta c/\sigma_1^2$ is a perturbation theory expansion parameter. **S** and **N** are, respectively, the signal and noise powers. The above expression provides a good approximation to the power spectral density for $\zeta < 1$ and has been derived under an adiabatic (i.e. low-frequency) approximation $\omega \ll U^{(2)}(c)$ that is somewhat less stringent than the $\omega \ll r_0$ approximation introduced earlier. The SNR is then obtained from

$$SNR = 10\log\left[\frac{1}{\mathbf{N}(\omega)}\left\{\frac{\mathbf{S}(\omega)}{\Delta\omega} + \mathbf{N}(\omega)\right\}\right], \tag{17}$$

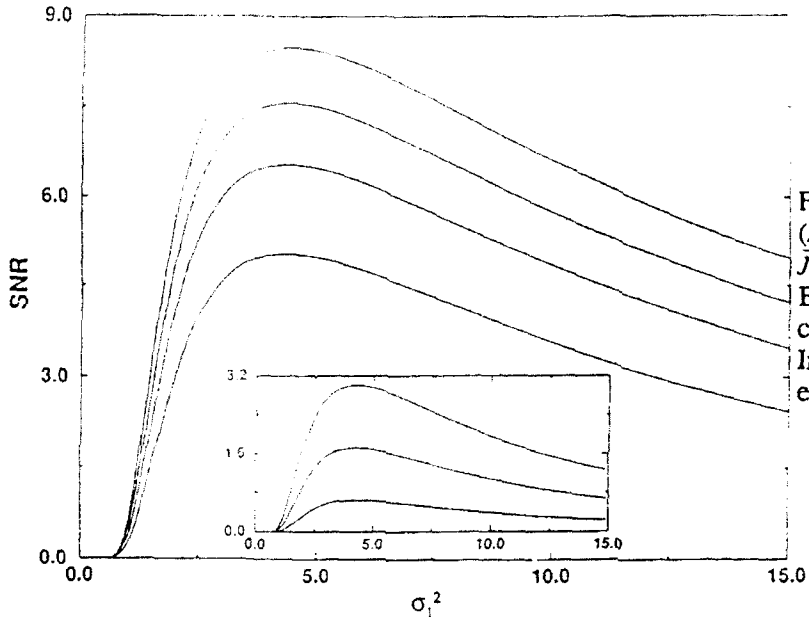

Fig 3. SNR computed from (16) and (17) for $(R_1, R_2, q, \omega, \Delta\omega, N) \equiv (10, 0.6, 0.1, 0.1, 0.001, 100)$. $\bar{J}_{1i} = 1 = -\bar{J}_{i1}, \overline{J_{i1}^2} = 1 = \overline{J_{1i}^2}, \bar{J}_{ii} = 0, \overline{J_{ii}^2} = 1, (i > 1)$. Bottom curve: $J_{1i} = 0$ (isolated case). Remaining curves: $\sigma_2^2 = 0$ (top), 1 (middle), and 2 (lower). Inset: the case for no modulation in the cell-body eqn. in the system (1).

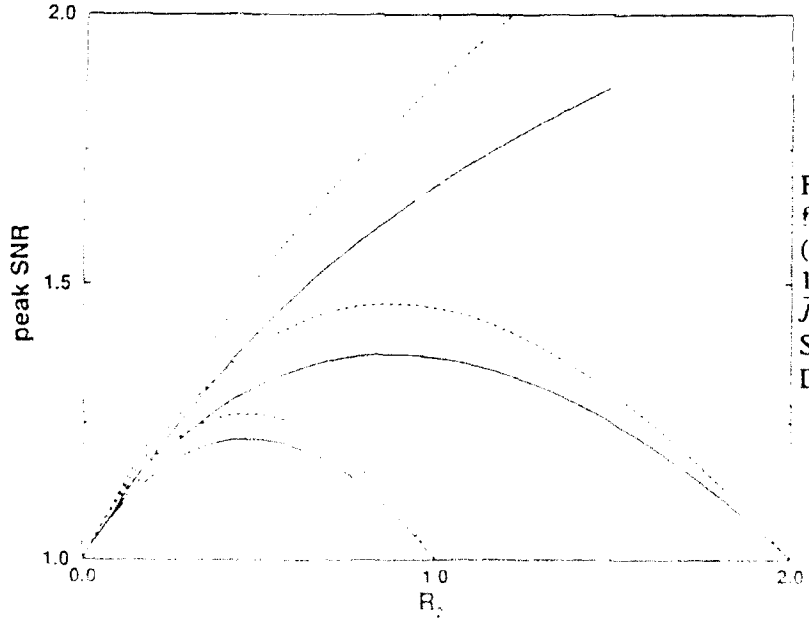

Fig 4. Peak SNR (normalized to its value for $J_{1i} = 0$ case) vs. R_2 for $(R_1, q, \omega, \Delta\omega, N) \equiv (10, 0.1, 0.1, 0.001, 10)$ and $\sigma_2^2 = 0$ (top curve), 1 (middle curve), 2 (bottom curve). $\bar{J}_{ii} = 0, \overline{J_{ii}^2} = 1, (i > 1)$. Solid curves: $\bar{J}_{1i} = 1 = \bar{J}_{i1}, \overline{J_{i1}^2} = 1 = \overline{J_{1i}^2}$. Dotted curves: $\bar{J}_{1i} = 1 = -\bar{J}_{i1}, \overline{J_{i1}^2} = 1 = \overline{J_{1i}^2}$.

absence of the bath, as a consequence.

IV. STATISTICAL ANALYSIS OF FIRING EVENTS

It is important to point out that stochastic resonance (as characterized by the bell-shaped SNR vs. noise variance curve of figure 3) has not yet been directly observed in a living system (although we will ennunciate a possible caveat to this statement at the end of the following subsection). The existence of noise-induced switching in the nervous system would seem, however, to be an eminently reasonable assumption, based on our simple model of the neuron as a noisy bistable switching element. Certainly, noise is ubiquitous in the nervous system; hence one might expect that when sensory neurons are periodically stimulated, the time intervals between successive firing events contain sensory information. These "reset" or "refractory" events correspond to the repolarization of the cell membrane. In fact, this has been well-known to neurophysiologists for many years. In neurophysiological experiments it is common to assemble an ensemble of firing events and fit a histogram to the intervals between the spikes. An example of these Inter-Spike-Interval Histograms (ISIHs), which are quite commonly seen in the neurophysiological literature, is shown in the following subsection. In this subsection we also demonstrate how the salient features of the experimentally observed ISIHs can be easily explained by our bistable model; in fact, we shall see that our model affords the *simplest possible* interpretation of the experimental spike train data. Throughout the rest of this work we show results for arbitrary values of the constants α, β, δ in (9), i.e., we do not consider the particular details of the quantities on the right-hand-sides of equations (11).

The Inter-Spike-Interval Histogram

We now return to our reduced system (9) and consider only the time intervals of the transitions between the potential wells (labeled A and B) while ignoring the intrawell motion (recall that the potential wells correspond, roughly, to the firing and refractory states of the soma). This is tantamount to replacing the detailed dynamics contained in (9) by the equivalent "two-state dynamics" depending only on the barrier height and the locations of the elliptic points of the potential (10). The result is the random "telegraph signal" $x(t)$ ($\equiv u_1(t)$ in the notation of this paper) depicted in figure 5.

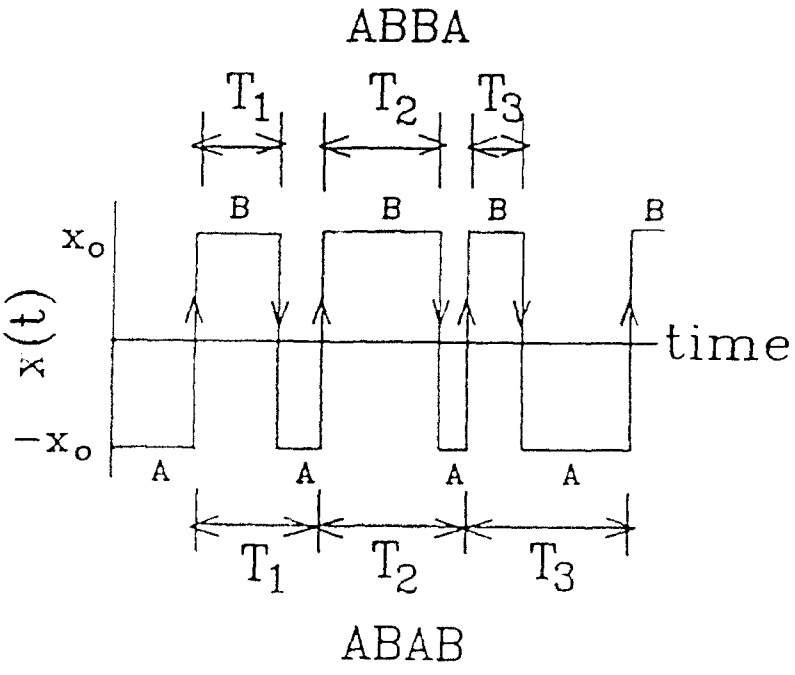

Fig 5. Sample output from two-state device driven by noise plus weak sinusoidal modulation. Stable states at $\pm x_0$ are labelled A and B. The ABBA and ABAB sequences shown, are the only consecutive time-interva sequences available to the two-state system from which ISIHs can be generated.

the deterministic modulation in (9), the two sequences of figure 5 lead to different ISIHs. The top sequence, referred to as the ABBA process, measures the escape time from well B. It leads to an ISIH with modes located at *odd integer multiples of T/2*, T being the modulation period. A theory describing this histogram has recently been developed [Zhou, Moss and Jung 1991]. The bottom sequence (the ABAB process) leads to a histogram with peaks located at *all integer multiples of T*. This is the sequence commonly observed in experiments (and the one that we concentrate on through the remainder of this discussion): it points to the existence of a "reset mechanism" between every pair of spikes. The reset events are identified with the repolarizations of the neuron membrane that occur between successive upstrokes of the action potential and are not directly observable in neurophysiological experiments. In figure 6 we show an experimental ISIH obtained from the single auditory nerve fiber of a cat. This data should be compared with the ABAB ISIH shown in figure 7. The sequence in this figure is obtained via analog simulation of (9) with the potential function U given by (10) as well as the "standard quartic" $U(u_1) = -\frac{1}{2}u_1^2 + \frac{1}{4}u_1^4$ (this potential is also bistable). The sequence of peaks in the ISIH implies a form of phase-locking of the neuron dynamics to the stimulus. Starting from its quiescent state, the neuron tries to fire at the first maximum of the stimulus cycle. If it fails to do so, it will fire at the next maximum of the stimulus (i.e. after a complete stimulus cycle) and so on, with a firing event corresponding to a switch between the two states of the potential (10). This "statistical skipping" leads to the sequence of peaks in the ISIH. Decreasing the noise strength (keeping all the other parameters fixed) leads to more peaks in the histogram since skipping becomes more likely. Conversely, increasing the noise tends to concentrate the probability into the first few peaks. For vanishingly small stimulus amplitude, the peaks merge into a Gamma distribution characterizing the ISIH for the spontaneous case [Longtin et. al. 1992]; such a distribution has also been observed experimentally.

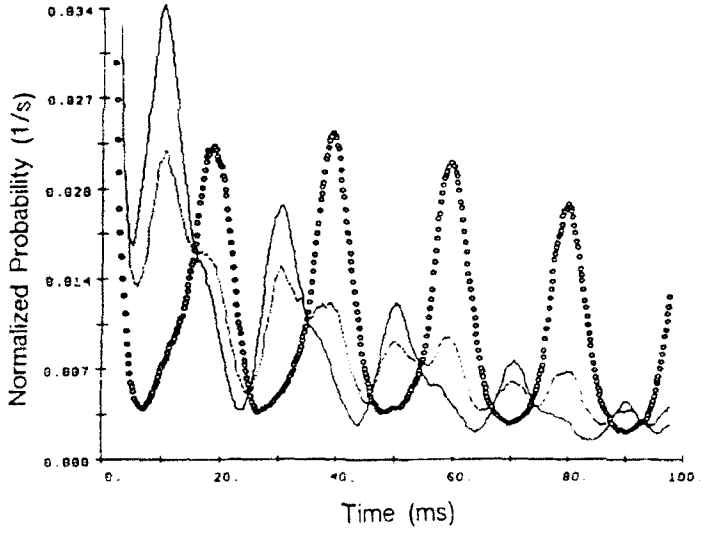

Fig 8. ISIHs computed via numerical simulation of (9) with $(\beta, q, \omega, \sigma_1^2) \equiv (1.6056, 0.304, \pi/10, 0.134)$ and uncertainty (see text) $\Delta t = 0$ (solid curve), 0.1 (dotted curve), and 0.25 (data points). Note the transition from peaks at $nT/2$ to peaks at nT for increasing Δt.

Our model is seen to reproduce all substantive features of the experimental data: in addition to the characteristic T-dependent locations of the successive peaks, the modal decay rates (except for the first few peaks) are exponential. Analog simulations show [Longtin, Bulsara and Moss 1991; Longtin et. al. 1992] that, on a semi-logarithmic scale, the decay constant is proportional to the modulation amplitude δ for fixed noise intensity σ_1^2, with a qualitatively similar relationship obtained between the decay rate and the noise strength for constant δ. This is not too surprising since the noise and signal are on equal footing in (9). We may then speculate that, over a certain (as yet not fully defined) range of parameters, the noise and signal play interchangeable roles in determining the shape of the ISIH. Their roles are not completely reciprocal, however, since the peak-widths in the ISIH are dependent on σ_1^2. Increasing the stimulus amplitude leads to an increase in the heights of the lower lying peaks. This is consistent with experimental observation

transcend our simple description. Clearly, this is an area which merits considerable further study.

Comparison to Integrate-Fire Models

A stochastic model, similar in spirit to the *deterministic integrate-fire model* (see e.g. Keener, Hoppensteadt and Rinzel 1981, and references therein) was originally developed (Gerstein and Mandelbrot 1964) to try to explain the experimentally observed ISIH corresponding to spontaneous firing events; as pointed out above, this distribution function is a Gamma distribution. Assuming the underlying dynamics to be time-stationary, a random walk description was invoked, based on the cornerstone requirement of a stable distribution function for the probability density of first passage times corresponding to the dynamics. The state variable u_1 was assumed to execute a biased random walk to an absorbing threshold at which point a firing event was designated to have occurred and the membrane potential u_1 was then instantaneously reset to its starting value (the reset mechanism being purely deterministic unlike our bistable model, in which it is stochastic). The distance between the origin and the threshold is the "barrier height" z (analogous to the height U_0 of the potential barrier in our bistable model) in the Gerstein-Mandelbrot description. Further, it was assumed that the motion in phase space occurs under the influence of a positive drift coefficient μ which was defined by Gerstein-Mandelbrot as the difference between the drift velocities corresponding to excitatory and inhibitory synaptic inputs (it is neurophysiologically reasonable to assume these velocities to be different). Then, assuming the presence of some (as yet unquantified) random background noise which is taken to be Gaussian delta-correlated with zero mean and variance σ^2, one may write down the Langevin equation for this process:

$$\dot{u}_1 = \mu + F(t), \tag{18}$$

to which corresponds the Fokker Planck equation

$$\frac{\partial}{\partial t} P(u_1, t) = -\mu \frac{\partial P}{\partial u_1} + \sigma^2 \frac{\partial^2 P}{\partial U_1^2}, \tag{19}$$

for the probability density function $P(u_1, t)$. This equation can be readily solved subject to the appropriate boundary conditions and the probability density function of first passage times written down in the form [Gerstein and Mandelbrot 1964],

$$g(t) = \frac{z}{\sqrt{2\pi\sigma^2 t^3}} \exp\left\{ -\frac{(z - \mu t)^2}{2\sigma^2 t} \right\}. \tag{20}$$

The density function $g(t)$ reproduces many of the properties of experimentally observed ISIHs for the spontaneous firing case. The mean first passage time to the absorbing threshold is calculated as the first moment of $g(t)$, and its reciprocal yields an average firing rate. Variations of this model incorporating moving boundaries (which mimic refractoriness and are therefore closer to neurophysiological reality) as well as a drift term that is linear in the dependent variable u_1 (the underlying dynamics is, in this case, representative of an Ornstein-Uhlenbeck process), have been studied by Johanessma [1968] and, Clay and Goel [1973].

In order to make even better contact with experimental results, it is necessary to provide reasonably good numerical values for the drift coefficient μ, the "barrier height" z and the background noise variance σ^2 in the above model. A first attempt to do so (while simultaneously providing a test of the goodness of fit of the model to neurophysiological data) was carried out by Berger et. al. [1990]. They carried out an experiment aimed at recording the inter-spike-interval distribution from extra-cellular recordings on the cat visual cortex. Having obtained the experimental ISIHs, they were able to compute the equivalent model quantities μ and z via the mean and standard deviation of the experimentally obtained ISIHs, assuming a fixed background noise variance σ^2. While we do not give any further details of the experiment, it is noteworthy that, once these "self-consistent" values of μ, z and σ^2 were substituted into the first passage time probability density function, an excellent fit of the model (20) to the experimental ISIHs resulted. In a subsequent publication, Berger and Pribram [1992] extended their work to incorporate the

the fully coupled N-body system within the constraints of the theory. The approach leads to a macroscopic "potential" function U (defined in (16)) which guarantees global stability of our dynamic system for positive α without having to constrain ourselves to a symmetric coupling matrix **J**. Our theory is seen to agree well with large numerical simulations of the coupled stochastic differential equations (1), within the bounds imposed by the constraints (2) and (12).

The theory described here enables us to describe a network of nonlinear oscillators with *nonlinear* coupling. However, because of the separation of time-scales, the dendritic bath is tacitly assumed to be very close to its steady state. This leads to the quasi-linearization approximations (9) and (11) and brings our description of the bath closer to other quasi-linear dendritic models [see e.g. Segev et. al. 1989]. In effect, we have assumed that the dendritic patches are only weakly bistable; they are not "strong" threshold devices. These assumptions also bring our approach closer to conventional mean-field theories [see e.g. Amit 1989 for an overview]. Unlike such theories, the current approach does not depend on a large number N of entities to improve its convergence although, as pointed out earlier, in the presence of additional elements in (1) with similar time constants, recourse to a more conventional mean-field approach may be unavoidable. Further, it is interesting to note that the notion of representing the dendritic bath as a tesselation of elemental volumes each described by a quasilinear stochastic differential equation for an activation function u_i $(i>1)$ is similar in spirit to existing compartmental models of dendritic trees (see e.g. Segev et. al. 1989). Our results appear to be independent of the choice of the statistics of the elements of **J**; repeating the calculations of this paper with the J_{ij} drawn from a uniform distribution yields qualitatively similar results although, as pointed out earlier, Gaussian statistics may be more reasonable from a neurophysiological perspective. In this connection it is worth pointing out that one expects typically small/sparse interactions (characterized by coefficients $J_{ij} \to 0$ $i,j > 1$) between dendritic volumes so that these coefficients may indeed be reasonably characterized by a sharply peaked (about zero mean) Gaussian. The distribution of the coefficients J_{1j} and J_{j1} (these coefficients characterize the interaction between the soma and the dendritic volumes) is broader. Good agreement between the probability density $P(u_1)$ for the reduced system (9) and the exact system (1) is also obtained for somewhat larger q values and noise strengths (within the bounds of the inequality (12)), although the agreement begins to break down when the adiabatic condition on the frequency is violated. The magnitudes and *signs* of the J_{ij} can be very important in determining the overall sign of the renormalized coefficient β in (11b) and this, in turn, determines the modality of the potential (10). For a monostable potential ($\beta < \alpha$) the cell body is always quiescent and there are no cooperative effects. The bath coupling can render a monostable potential (for the isolated cell body) bistable, under certain conditions, thereby imparting a firing capability to the neuron; the opposite effect can also occur. This is evident from the definitions (11b,c): changing the dendritic parameters changes the barrier height and the location of the elliptic points of the effective potential (10) that characterizes the soma dynamics, while also renormalizing the modulation amplitude. These changes lead, in turn, to changes in the SNR given by the expressions (16) and (17).

The approach to the processing of information in noisy nonlinear dynamical systems, based on the probability density of residence times in one of the stable states of the potential offers an alternative to the FFT, and has been applied [Longtin, Bulsara and Moss 1991; Longtin et. al. 1992] in the theoretical construction of inter-spike-interval histograms (ISIHs) that describe neuronal spike trains in the central nervous system. This model exhibits remarkable agreement with data obtained in two different experiments some 25 years apart [Rose et. al. 1967; Siegal 1990] as well as with the more recent data of Rhode [1991; unpublished]; figures 6 and 7 demonstrate this agreement. The approach of Longtin et. al. has been contrasted with more conventional theories of ISIHs based on integrate-and-fire (IF) models in which the activation performs a random walk to an absorbing barrier and is then reset to its initial value. In the absence of an absolute retractory period, the two approaches may, in fact, converge with the mean firing rate (computed as the reciprocal of the mean first passage time) in the IF model corresponding, roughly, to the mean duration of a full-cycle switching event in the bistable diffusion model of Longtin et. al. The approach of Longtin et. al., however, seems to offer the most elegant treatment of the ISIH, certainly it permits one to match the model with experimental data (far more closely than

REFERENCES

Abbott LF, Kepler TB (1990) Model neurons: from Hodgkin-Huxley to Hopfield. In Garrido L. (ed.) Statistical mechanics of neural networks. Springer, Berlin

Amit DJ (1989) Modeling brain function. Cambridge Univ. Press, Cambridge

Berger D, Pribram K, Wild H, Bridges C (1990) An analysis of neural spike-train distributions: determinants of the response of visual cortex neurons to changes in orientation and spatial frequency. Exp. Brain Res. 80:129-134.

Berger D, Pribram K (1992) The relationship between the Gabor elementary function and a stochastic model of the inter-spike-interval distribution in the responses of visual cortex neurons. Biol. Cyb. 67:191-194.

Buhmann J, Schulten K (1986) Influence of noise on the behavior of an autoassociative neural network. In Denker J (ed.) Neural networks for computing. AIP, New York.

Buhmann J, Schulten K (1987) Influence of noise on the function of a "physiological" neural network. Biol. Cyb. 61:313-327.

Bulsara AR, Boss RD, Jacobs EW (1989) Noise effects in an electronic model of a single neuron. Biol. Cyb. 61:211-222.

Bulsara AR, Schieve WC (1991) Single effective neuron: macroscopic potential and noise-induced bifurcations. Phys. Rev. A44:7913-7922.

Bulsara AR, Jacobs EW, Zhou T, Moss FE, Kiss L (1991a) Stochastic resonance in a single neuron model: theory and analog simulation. J. Theor. Biol. 152:531-555.

Bulsara AR, Maren AJ, Schmera G, (1992) Single effective neuron: dendritic coupling effects and stochastic resonance. Biol. Cyb., preprint.

Chialvo DR, Apkarian AV (1992) Modulated noisy biological dynamics: three examples. In Shlesinger MF, Moss FE, Bulsara AR (eds.) Proceedings of the NATO Advanced Research Workshop on Stochastic Resonance and its Applications to Physics and Biology; to appear.

Clark JW (1988) Statistical mechanics of neural networks. Phys. Repts. 158:91-157.

Clark JW (1989) Introduction to neural networks. In Proto AN (ed.) Nonlinear phenmoena in complex systems. North Holland, Amsterdam.

Clay JR, Goel NS (1973) Diffusion models for the firing of a neuron with varying threshold. J. Theor. Biol. 39:633-644.

Cowan JD (1970) A statistical mechanics of nervous activity. In Gerstenhaber M (ed.) Some mathematical questions in biology. Amer. Math. Soc., Providence, RI.

Cowan JD (1974) Stochastic models of neuro-electric activity. In Rice SA, Freed KF, Light JC (eds.) Statistical mechanics. Univ. of Chicago Press, Chicago.

Cox DR, Miller HD (1972) Theory of stochastic processes. Chapman and Hall, London.

Eccles JC (1964) The physiology of synapses. Academic Press, N.Y.

(eds.) Proceedings of the NATO Advanced Research Workshop on Stochastic Resonance and its Applications to Physics and Biology; to appear.

Maren AJ, Harston CT, Pap RM (1990) Handbook of neural computing applications. Academic Press, San Diego, California.

McNamara B, Wiesenfeld K (1989) Theory of stochastic resonance. Phys. Rev. A39:4854-4869.

Nicolis G, Nicolis C, McKeman D (1992) Stochastic resonance in chaotic dynamics. Shlesinger MF, Moss FE, Bulsara AR (eds.) Proceedings of the NATO Advanced Research Workshop on Stochastic Resonance and its Applications to Physics and Biology; to appear.

Moss FE (1992) Stochastic resonance; from the ice ages to the monkey's ear. In Weiss G (ed.) Some problems in statistical physics. SIAM, Philadelphia.

Pribram K (1991) Brain and perception: holonomy and structure in figural processing. Lawrence Erlbaum Assoc., Hillsdale, NJ.

Rall W (1970) Dendritic neuron theory and dendro-dendritic synapses in a simple cortical system. In Schmidt FO (ed.) The neurosciences: second study program. Rockefeller Univ. Press, New York.

Rall W, Rinzel J (1973) Branch input resistance and steady state attenuation for input to one branch of a dendritic neuron model. Biophys. J. 13:648-688.

Rinzel J, Rall W (1974) Transient response in a dendritic neuron model for current injcted at one branch. Biophys. J. 14:759-790.

Rinzel J, Ermentrout B (1989) Analysis of neuronal excitability and oscillations. In Koch C, Segev I (eds.) Methods in neuronal modeling. MIT Press, Cambridge, Mass.

Risken H (1984) The Fokker Planck equation. Springer, Berlin.

Rose J, Brugge J, Anderson D, Hind J (1967) Phase-locked response to low frequency tones in single auditory nerve fibres of squirrel monkey. J. Neurophys. 30:769-793.

Schieve WC, Bulsara AR, Davis G (1991) Single effective neuron. Phys. Rev. A43:2613-2623.

Segev I, Fleshman JW, Burke RE (1989) Compartmental models of complex neurons. In Koch C, Segev I (eds.) Methods in neuronal modeling. MIT Press, Cambridge, Mass.

Segev I, Rapp M, Manor Y, Yarom Y (1992). Analog and digital processing in single nerve cells: dendritic integration and axonal propagation. In McKenna T, Davis J, Zornetzer S (eds.) Single neuron computation. Academic Press, N.Y.

Siegal R (1990) Nonlinear dynamical system theory and primary visual cortical processing. Physica 42D:385-395.

Stein RB (1967) Some models of neuronal variability. Biophys. J. 7:37-68.

Stein RB (1965) A theoretical analysis of neuronal variability. Biophyshys. J. 5:173-184.

Stein RB, Leung KV, Oguztoreli MN, Williams BW (1974) Properties of small neural networks Kybernetik 14:223-230